Microchim Acta (2014) 181:663–670
DOI 10.1007/s00604-014-1171-3

ORIGINAL PAPER

Aptamer based test stripe for ultrasensitive detection of mercury(II) using a phenylene-ethynylene reagent on nanoporous silver as a chemiluminescence reagent

Fang Liu · Shoumei Wang · Meng Zhang · Yanhu Wang · Shenguang Ge · Jinghua Yu · Mei Yan

Received: 21 November 2013 / Accepted: 14 January 2014 / Published online: 28 January 2014

Abstract We describe a paper-based chemiluminescence (CL) test for the determination of mercury(II) ion. A single-stranded DNA aptamer was first covalently immobilized via its amino groups to the hydroxy groups on the surface of cellulosic paper. The aptamer probes can capture Hg(II) ions due to their specific interaction with thymine. The CL reagent (a caboxylated phenylene-ethynylene referred to as P-acid) was immobilized on nanoporous silver (NPS@P-acid) and used a CL label on the aptamer. The stripe is then contacted with a sample containing Hg(II) ions and CL is induced by the addition of permanganate. CL intensity depends on the concentration of Hg(II) because Hg(II) increases the quantity of the P-acid-conjugated aptamer. The highly active surface of the NPS@P-acid composites results in an 8-fold higher CL intensity compared to the use of pure P-acid. This enables Hg(II) ion to be quantified in the 20 nM to 0.5 μM concentration range, with a limit of detection as low as 1 pM. This CL aptasensor is deemed to represent a promising tool for simple, rapid, and sensitive detection of Hg(II).

Keywords Chemiluminescence · Aptasensor · Lab on paper · Nanoporous silver · P-acid

Electronic supplementary material The online version of this article (doi:10.1007/s00604-014-1171-3) contains supplementary material, which is available to authorized users.

F. Liu · S. Wang · M. Zhang · Y. Wang · S. Ge · J. Yu (✉) · M. Yan
Key Laboratory of Chemical Sensing & Analysis in Universities of Shandong, School of Chemistry and Chemical Engineering, University of Jinan, Jinan 250022, China
e-mail: ujn.yujh@gmail.com

Introduction

The monitoring of toxic metal ions in aquatic ecosystems is an important issue because of its adverse effect on human health and the environment [1]. Mercury (II) ion (Hg(II)), one of the most potently toxic metal ions, can cause severe irreversible harm to the human body mainly via the central nervous system, digestive system, and internal organs [2]. Furthermore, the Hg(II), arised from a variety of sources (such as oceanic, volcanic emissions, gold mining, the combustion of solid waste and fuels) is widely distributed in atmosphere, water, and soil. And this prompted the development of new methods for Hg(II) determination with great simplicity, high sensitivity and good selectivity [3]. Up to now, numerous methods have been developed for Hg^{2+} determination, such as inductively coupled plasma mass spectrometry [4], atomic absorption spectroscopy [5], atomic fluorescence spectroscopy [6], and electrochemical methods [7]. However, most of them require expensive and sophisticated instrumentation, skilled operator, and complex sample pre-processing, and they cannot be used for on-site determination of Hg(II) in the environment.

Aptamers, first introduced by three groups independently in 1990 are the artificial single-stranded DNA or RNA sequences, that can recognize target molecule (small molecules, proteins, and even entire cells) with extremely high specificity [8–10]. Hg(II) can specifically interact with thymine-rich DNA sequences (called Hg(II) aptamers) to form thymine–Hg(II)–thymine (T–Hg(II)–T) complexes [11]. The use of aptamer opens a new field for highly sensitive and simple determination of Hg(II) due to its inherent advantages of high stability, easy storage, easy modification, and high affinity. Nowadays, many biosensors combined with surface plasmon resonance (SPR) spectroscopy [12], colorimetric assays [13],

fluorescence detection [14], and electrochemical transducers [15] have been developed for Hg(II) determination. However, the limit of detection (LOD) and analysis time are often cited as problems in the Hg(II) determination. Therefore, chemiluminescence (CL) is considered as a promising alternative to resolve the above-mentioned problems, because of its high sensitivity, wide linear range, simple instrumentation, and no background scattering light interference.

We describe here, a novel CL aptasensor is designed to realize the simple and on-site determination of Hg(II) by incorporating the aptamer recognition elements onto the recently developed microfluidic paper-based analytical devices. So our method can combine the advantages of paper-based tests and conventional lab-on-chip devices [16, 17]. Paper, a three-dimensional cellulose fiber web with high surface area, is an attractive substrate for microfluidic devices. This can be due to its various unique advantages: cheap, abundant, easy to use and disposable, convenient to store, transport, modify, and able to move fluids by capillary action without an external power source. Hydrophilic channels are patterned on paper by hydrophobic walls of photoresist/polymer, inks, wax, and plasma treatment, laser treatment or by cutting method [18–21]. N,N'-carbonyldiimidazole (CDI), containing two acylimidazole leaving groups, was used as a novel simple crosslinker strategy to covalently immobilize the aptamer on the paper test strip without any spacer molecules. CDI can react with hydroxyl groups to create a reactive intermediate-imidazolyl carbamate. Then the reactive intermediate can be coupled to amine-containing molecules with the result of a one-carbon spacer, forming stable urethane (N-alkyl carbamate) linkages. Thus, CDI was employed as viable alternatives to traditional crosslinker (such as periodate and chitosan) in our previous work [22] due to its simple fabrication procedures. The covalent coupling of aptamers on a paper device display high binding stability for regeneration and reusability for the further development of low-cost application. Therefore, a novel CL system based on the CDI modified paper and phenylene-ethynylene derivative (4,4′-(2,5-dimethoxy-1,4-phenylene)bis (ethyne-2,1-diyl) dibenzoic acid) (P-acid)-potassium permanganate ($KMnO_4$) system was designed. And the figure with the chemical formula of P-acid was added in Fig. 1. We describe here, the P-acid was selected as the CL signal labeling for the first time.

Recently, nanoporous silver (NPS) with controllable three-dimensional (3D) structure, high surface-to-volume ratio, good stability, and nice biocompatibility has roused great interest [23, 24]. Due to its advantages, NPS was used to conjugate with P-acid (formed NPS@P-acid composite) for signal amplification strategy. In the presence of Hg(II), the aptamer probe folds into T–Hg(II)–T mediated hairpin structure, and the NPS@P-acid labeled on aptamer can provide a readout signal for quantitative determination of Hg(II). The system using NPS@P-acid composites exhibit 8-fold enhancement of CL intensity as compared to that based on pure P-acid, revealing a more sensitive sensor for Hg(II) determination. Herein, the LOD as low as 0.01 nM for Hg(II) was obtained under optimal experimental conditions. Furthermore, the system was further applied to the determination of Hg(II) in river water samples with satisfactory results. This paper-based CL aptasensor will be a promising candidate for on-the-spot detection of Hg(II) in real environmental samples.

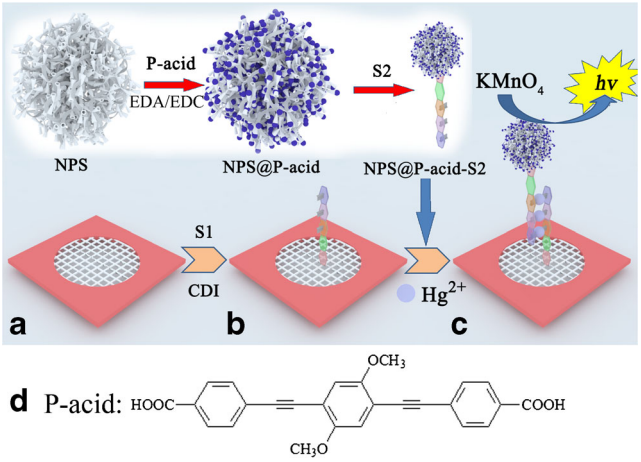

Fig. 1 Schematic representation of the fabrication process of paper-based CL device. **a** paper working zone; **b** the paper was modified with CDI and aptamer; **c** after immobilized with NPS@P-acid and capturing with Hg^{2+}; **d** the picture with chemical formula of P-acid

Materials and methods

Reagents and materials

Tween-20, N,N'-carbonyldiimidazole (CDI), N-(3-dimethylaminopropyl)-N'- ethylcarbodiimidehydro-chloride (EDC), NaOH, ethylenediamine (EDA) were obtained from Sigma (St. Louis, MO, USA, http://www.sigmaaldrich.com). $KMnO_4$, ethanol and ethanolamine were obtained from Alfa Aesar China Ltd (http://alfa.com/china). $Ag_{23}Al_{77}$(at.%) alloy precursors were fabricated by melt-spinning, which generated thin foils with thickness of about 50 μm. Whatman chromatography paper 1 (200.0 mm×200.0 mm) (pure cellulose paper) was purchased from GE Healthcare World-wide (Pudong Shanghai, China, http://www3.gehealthcare.com/en/Global_Gateway). This type of Whatman paper was chosen because of its uniform composition (relative to other types of paper) and lack of additives that affect flow rate and CL reaction. The DNA oligonucleotide sequences shown below were purchased from Shanghai Linc-Bio Science Co. LTD (Shanghai, China, http://lincbio.cn.china.cn/).

(S1) 5′-NH_2-$(CH_2)_6$-CAGTTTGGAC-3′

(S2) 5′-NH_2-GTCCTTTCTG-3′

0.05 % Tween-20 was spiked into 0.1 M pH 7.4 PHOSPHATE BUFFER as washing buffer. Ultrapure water obtained from a Millipore water purification system (≥18 MΩ·cm, Milli-Q, Millipore) was used in all assays and solutions.

The scanning electron microscopy (SEM) images were obtained from a QUANTA FEG 250 thermal field emission SEM (FEI Co., USA, http://www.fei.com/). CL emission was measured using a computerized ultraweak luminescence analyzer (Type RFL-200, manufactured at Xi'an Remex Analysis Instrument Co, Ltd, Xi'an, China, http://ccn.mofcom.gov.cn/1096057). The FT-IR spectra were performed on Thermo Scientific Nicolet 380 FT-IR spectrometer (Shanghai Keduo Co, Ltd, Shanghai, http://194127.ccen.net/). UV–Vis experiments were performed with a UV-3900 spectrophotometer (Hitachi, Japan, http://www.hitachi.com/). The contact angle tests were performed on contact angle measurement (Model OCA40, Dataphysics, http://www.dataphysics.com/zh).

Preparation of NPS@P-acid conjugated aptamer probe

According to the reported method [23], the NPS was prepared by dealloying the $Ag_{23}Al_{77}$ alloy foils in 1 M NaOH solutions for 72 h at 30 °C, followed by rinsing thoroughly with pure water. P-acid, first demonstrated the CL behavior with $KMnO_4$, was employed here and it was prepared according to the published literature [25].

To obtain the NPS@P-acid composites, 1 mg NPS nanoparticles and 1 mL EDA were dispersed in 3 mL ethanol by sonication for 10 min. After washing with 3 mL phosphate buffer (pH 7.4) and being centrifugal separated, the amino group functionalized NPS nanoparticles were added into 3 mL anhydrous solution of P-acid (4 mM) containing 5 mM EDC by sonication for 10 min. EDC, as the linking agent, can react with carboxy group to form an active acylimidazole group capable of coupling with amine-containing molecules [26]. After rinsing with ultrapure water thoroughly, the formed NPS@P-acid composites were immediately redispersed into 200 μL of 5 μM thiolated DNA aptamer (S2) solution. Then the mix was sonicated, and incubated for 30 min at room temperature to form the NPS@P-acid conjugated aptamer probe (S2). It has been proven that amino group and thiol group can be bound strongly to Ag [27]. The resulting aptamer probe were washed with phosphate buffer (pH 7.4) and then dispersed in phosphate buffer and stored at 4 °C before use.

Fabrication of the paper-based CL aptasensor

Fabrication details of this chemiluminescence (CL) paper test strip can be found in the supplemental information. As shown in Fig. 1, the fabrication process of CL aptasensor was constructed as follows: First, the paper zone was activated by adding 5 μL 0.3 M CDI for 5 min, and then washed sequentially with anhydrous ethanol, ice-cold water and phosphate buffer (pH 7.4) to remove excess CDI and reaction by-products. Then 10 μL of 5 μM aptamer probe (S1) solution was added on the paper zone, and reacted at room temperature for 10 min. Subsequently, excess aptamer probe (S1) was washed out with phosphate buffer containing 0.05 v/v Tween-20. And 5 μL 1 M ethanolamine was added and incubated for 5 min at room temperature to quench the remaining active groups. After washing with phosphate buffer containing 0.05 v/v Tween-20, the resulting CL aptasensor was obtained and stored at 4 °C before use.

Determination of Hg^{2+}

The procedures of Hg^{2+} determination on paper-based CL aptasensor were similar to our previous work [28], and a detailed procedure is described below. The determination of Hg^{2+} was performed by first adding 5 μL of Hg^{2+} solution with different concentration to the paper zone, then added 10 μL NPS@P-acid conjugated aptamer probe (S2), incubating for 15 min. After washing with phosphate buffer (pH 7.4), CL experiments were carried out through sequential injection of the p-acid-$KMnO_4$ system by a pipette according to the protocol reported in our previous work [22]. The CL signals related to the Hg^{2+} concentrations can be measured.

Results and discussion

Characterization of NPS, NPS@P-acid

The morphology of the NPS and the NPS@P-acid composites were characterized by the SEM images. As shown in Fig. 2a, it was observed that the ligament and nanopore channels were uniformly distributed across the entire sample. And the average size of the smooth silver ligament was about 30 nm. The 3D nanoporous material provided a flexible substrate for further functionalization. In addition, a slightly coarsened ligament size of 50 nm in Fig. 2b demonstrated the fact that P-acid can be immobilized on the NPS through ethanediamine cross-linking.

Characterization of NPS@P-acid conjugated aptamer probe

Figure 3a illustrates the formation of the NPS@P-acid composites and the NPS@P-acid conjugated aptamer probe. It can be seen from Fig. 3a that there were two obvious absorption peaks of P-acid, while no absorption peak was observed for the NPS. After NPS conjugated with P-acid, two distinct adsorption peaks were observed on the UV–Vis spectra of NPS@P-acid composites, which attributed to the adsorption peaks of P-acid. In addition, the adsorption peak from DNA

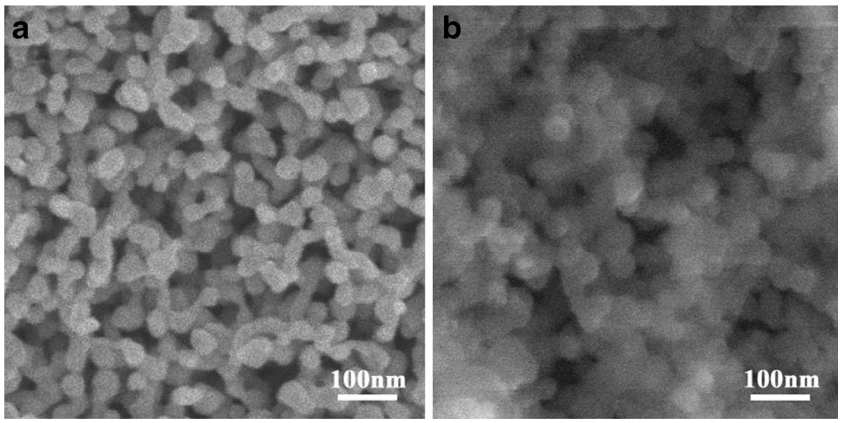

Fig. 2 Representative SEM images of **a** NPS; **b** NPS@P-acid composites

aptamer was about at 260 nm, and the obtained NPS@P-acid conjugated aptamer probe showed another obvious adsorption peak. And this confirmed the formation of the NPS@P-acid conjugated aptamer probe.

Characterization of the paper-based aptasensor device

Fourier Transform Infrared Spectroscopy (FTIRS) shown in Fig. 3b was used to confirm the immobilization of the NPS@P-acid conjugated aptamer probe on the paper zone. The absorption in curve B at 1,760 and 1,660 cm^{-1} can be assigned to the imidazole ester $\nu_{C=O}$, and the C = C and C = N stretching modes of the imidazole heterocycle of CDI. Due to the C = O stretching and NH deformation, the peaks at 1,740 and 1,530 cm^{-1} were observed in curve C with the disappearance of the absorptions at 1,760 and 1,660 cm^{-1}. So we can conclude the successful immobilization of the amino functionalized NPS@P-acid conjugated aptamer probe on CDI activated paper zone.

A pure cellulose paper was used as the substrate for the paper-based CL aptasensor device, and the morphology of the porous structures of paper electrodes were shown by SEM images in Fig. 4. The porous structure and microfibres of pure cellulose paper zone were shown in Fig. 4a and b. Due to the 3D porous structure of paper, when the wax screen-printed paper were baked, the melted wax would permeate into the paper, and hydrophobic walls were then fabricated (Fig. 4c and d). After CDI was modified on the wax-patterned paper, the surface of the paper was smoother than the wax penetrated one and the fiber was thicker than the pure cellulose paper (Fig. 4e and f). The contact angle on the front and back side wax-penetrated surface is 126° and 118°, respectively. Wax-screen-printing did not leave any contamination on hydrophilic paper zones. And after the curing process, the unprinted area maintained good hydrophilicity, flexibility, 3D porous structure and their original property as well. As shown in Fig. 4g and h, the surface of the paper was coated with some granular NPS after reaction, and 3D porous structure of the paper was not changed.

Kinetic characteristics of CL response on paper-based aptasensor device

Compared to the P-acid labeled aptamer probe, the CL response of the as-prepared paper-based NPS@P-acid tagged aptasensor was investigated to confirm the feasibility of CL reaction on wax-printed paper zone. As shown in Fig. 5a, the pure aptamer exhibited weak CL response (curve 1), and the

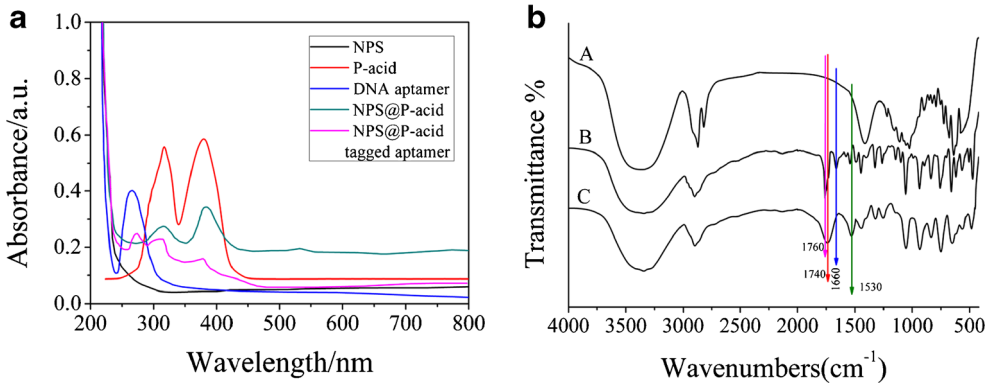

Fig. 3 **a** UV–Vis absorption of NPS@P-acid conjugated aptamer; **b** FTIRS of (curve A) original paper; (curve B) NPS@P-acid composites; (curve C) NPS@P-acid conjugated aptamer

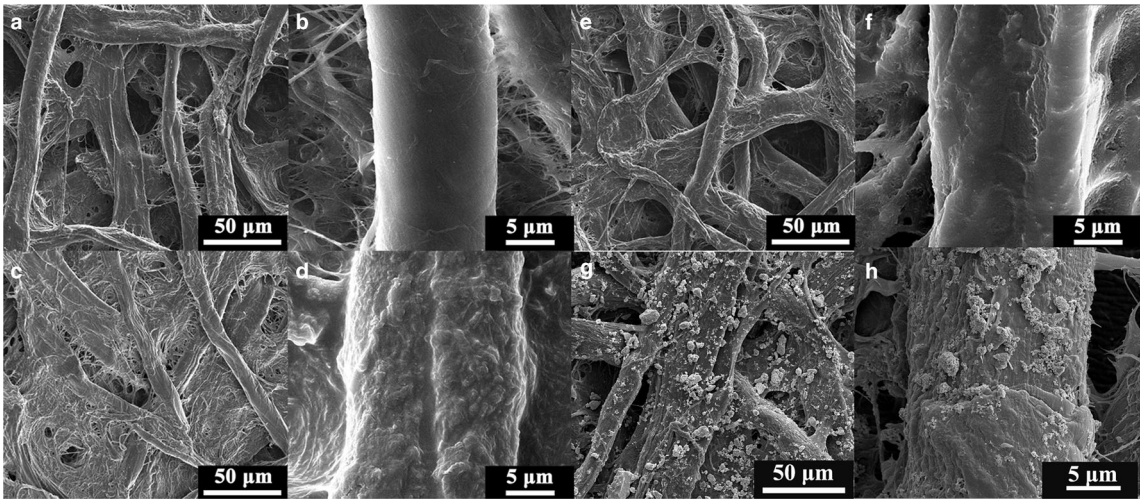

Fig. 4 Representative SEM image of **a**, **b** pure cellulose paper; **c**, **b** wax-printed paper; **e**, **f** CDI modified wax-penetrated paper

signal intensity of the NPS@P-acid (curve 3) was greatly increased compared with the P-acid (curve 2) under the same conditions, which indicated the enhanced sensitivity. The improved CL performance for our method can be due to a higher number of P-acid molecules loaded on the NPS to label the aptamer probe to achieve the signal amplification. In addition, the obtained signal increased with the increasing concentration of the analytes. Therefore, our paper-based aptasensor exhibited a good analytical performance for the Hg(II) determination and can be used in real sample.

The effect on CL sensor performance with different size of NPS

According the reported method [23], the NPS with different pore diameter can be prepared by dealloying the $Ag_{23}Al_{77}$ alloy foils in 1 M NaOH solutions for different time. To obtain optimum pore diameter, the dealloying time varied from 36 to 96 h, and the different CL sensor performance were shown in Figure S2A. From Figure S2, when the dealloying time varied from 36 to 96 h, the optimum CL performance was obtained at

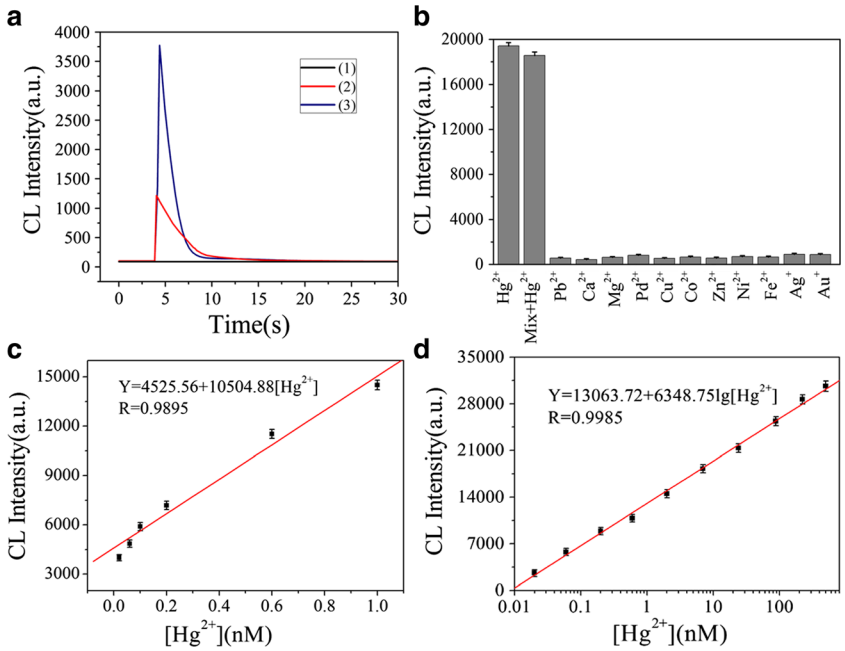

Fig. 5 **a** Kinetic characteristics of CL response on (1) pure aptamer; (2) P-acid; (3) NPS@P-acid composites under the same conditions; **b** Specificity with divalent metal ions (such as Pb^{2+}, Ca^{2+}, Mg^{2+}, Pd^{2+}, Cu^{2+}, Co^{2+}, Zn^{2+}, Ni^{2+}, Fe^{2+}, Ag^{+}, Au^{3+}). *Error bars* represent the standard deviations of measurements taken from at least five independent experiments; **c** The calibration curves of the paper-based CL aptasensor for Hg^{2+} determination in a low concentrations from 0.02 to 1 nM; **d** The calibration curves of the paper-based CL aptasensor for Hg^{2+} determination in the wide range from 0.02 to 500 nM. *Error bars* showed the standard deviations of six measurements

the dealloying time of 72 h. The pore diameter distribution for NPS at the dealloying time of 72 h was obtained according to the reported method [29], and the result with most pore diameter of 50 nm was shown in Figure S2B.

Selectivity, stability and reproducibility of the paper-based aptasensor device

Furthermore, the selectivity of the present paper-based aptasensor was tested for 10 nM Hg(II) over other metal ions such as Pb^{2+}, Ca^{2+}, Mg^{2+}, Pd^{2+}, Cu^{2+}, Co^{2+}, Zn^{2+}, Ni^{2+}, Fe^{2+}, Ag^{+} and Au^{3+}, at 4 mM concentration under the optimum conditions, respectively. As shown in Fig. 5b, the resulting paper-based aptasensor exhibited remarkable CL intensity only in the presence of Hg(II) rather than other metal ions, indicating good selectivity for the Hg(II) detection. Likewise, the device's CL response to Hg(II) was unaffected by the presence of mixture of metal ions.

When this paper-based aptasensor device was stored at 4 °C in a dry environment for over 1 month and it was used to measure the same Hg(II) concentration. The CL intensity of the paper-based aptasensor device was decreased to 91 % of its initial response, indicating the acceptable stability and suitability for storage or long-distance transport to remote regions and developing countries.

Reproducibility is also an extremely important feature for the paper-based aptasensor. The reproducibility was investigated by repetitive measuring of 10 nM Hg(II) in 11 individual strategies. And the relative standard deviation (RSD) of the reproducible CL response was 6.2 %, showing the good reproducibility of the protocol.

Performance of the paper-based aptasensor for Hg^{2+} determination

To evaluate the sensitivity of our method, the CL intensity of the novel paper-based aptasensor device was measured with various concentrations of Hg^{2+} ions. And the CL intensity was very sensitive to the change of the Hg^{2+} concentration. The enhanced CL intensity was linear in the low Hg^{2+} concentrations from 0.02 to 1 nM, and the equation of the calibration curve was I_{CL}=4,525.56+10,504.88 [Hg^{2+}] ([Hg^{2+}]/nM)(R=0.9895). And CL signal was logarithmically proportional to the Hg^{2+} concentration in the wide range from 0.02 to 500 nM, and the equation of the calibration curve was I_{CL}= 13,063.72+6,348.75 lg[Hg^{2+}] ([Hg^{2+}]/nM)(R=0.9985). In addition, the detection limit for Hg^{2+} was 0.01 nM at a signal-to-noise ratio of 3, indicating that the method can be used for the ultrasensitive determination of Hg^{2+}. The characteristics of various method for the determination of Hg^{2+} are summarized in Table 1. Compared with the other methods, the method has a wide linear range and a lower detection limit.

Table 2 Application of Hg^{2+} in real samples

Sample no.	Added (nM)	Found[a] ± S.D. (nM)	RSD (%)	Recovery (%)
1	0.00	0.00	–	–
2	2.50	2.56±0.05	1.95	102.4
3	5.00	5.03±0.12	2.38	100.6
4	7.50	7.27±0.16	2.20	96.9
5	10.0	9.98±0.15	1.50	99.8

[a] Average of five measurements

Application of the paper-based aptasensor in real samples

To further explore the practical applicability of the paper-based aptasensor device, the Hg(II) detection was conducted in water samples from the Yellow River, a realistically complex sample containing a variety of interferences. After filtering with 0.2 mm membrane to remove the insoluble substances, the samples were spiked with target Hg(II) over the range of 0.0–10 nM. As shown in Table 2, the recovery was between 96.9 and 102.4 %, which indicated that the system allowed the accurate quantification of Hg(II) in real samples without any interference from other potentially coexisting metal ions.

Conclusion

In summary, an ultrasensitive paper-based CL aptasensor was developed for Hg(II) determination based on the simplicity

Table 1 Comparison of major characteristics of different methods

Methods	Reagent	Dynamic range (nM)	LOD (nM)	References
Fluorescence	Mn:CdS/ZnS quantum dots	1–10	0.18	[30]
Electrochemical	Oligonucleotide	100–2,000	100	[31]
Spectrophotometry	C[6]/SiO2/CdTe nanoparticles	2–14	1.55	[32]
Surface-enhanced Raman scattering	Mesna modified Ag NPs	10–2,000	2.4	[33]
Chemiluminescence	Luminol-H_2O_2	5–500	4	[34]
Chemiluminescence	nanoporous Ag@phenylene-ethynylene	0.2–500	0.01	This work

and low-cost of paper test strip and the selectivity of the aptamer. This assay allows us to determine Hg(II) down to 0.1 nM. The main advantages are as follows: First, the aptamer was covalently immobilized on the paper zone through CDI covalent crosslinking with simple fabrication procedures. Second, P-acid, first demonstrated a well-defined CL response with $KMnO_4$, was selected as the CL reagent we describe here. The as-prepared NPS@P-acid composites were used as signal label with signal amplication technique. This low-cost, sensitive, stable, rapid biosensor can detect Hg(II) in real samples, which are well suited for facile on-site and real-time determination of Hg(II) in biological and environmental monitoring. It supplies a promising platform for detecting other metal ions by replacing the other metal-dependent aptamer.

Acknowledgments This work was financially supported by Natural Science Research Foundation of China (21277058, 21175058, 21207048) and Natural Science Foundation of Shandong Province, China (ZR2012BZ002).

References

1. Nolan EM, Lippard SJ (2008) Tools and tactics for the optical detection of mercuric ion. Chem Rev 108:3443–3480
2. Vupputuri S, Longnecker MP, Daniels JL, Guo X, Sandler DP (2005) Blood mercury level and blood pressure among US women: results from the National Health and Nutrition Examination Survey. Environ Res 97:195–200
3. Virtanen JK, Rissanen TH, Voutilainen S, Tuomainen TP (2007) Mercury as a risk factor for cardiovascular diseases. J Nutr Biochem 18:75–85
4. Malinovsky D, Sturgeon RE, Yang L (2008) Anion-exchange chromatographic separation of Hg for isotope ratio measurements by multicollector ICPMS. Anal Chem 80:2548–2555
5. Nguyen TH, Boman J, Leermakers M, Baeyens W (1998) Mercury analysis in environmental samples by EDXRF and CV-AAS. Fresenius J Anal Chem 360:199–204
6. Gomez-Ariza JL, Lorenzo F, Garcıa-Barrera T (2005) Comparative study of atomic fluorescence spectroscopy and inductively coupled plasma mass spectrometry for mercury and arsenic multispeciation. Anal Bioanal Chem 382:485–492
7. Gong J, Zhou T, Song D, Zhang L, Hu X (2010) Monodispersed Au nanoparticles decorated graphene as an enhanced sensing platform for ultrasensitive stripping voltammetric detection of mercury (II). Anal Chem 82:567–573
8. Tuerk C, Gold L (1990) Systematic evolution of ligands by exponential enrichment: RNA ligands to bacteriophage T4 DNA polymerase. Science 249:505–510
9. Ellington AD, Szostak JW (1990) Selection in vitro of single-stranded DNA molecules that fold into specific ligand-binding structures. Nature 346:818–822
10. Robertson DL, Joyce GF (1990) Selection in vitro of an RNA enzyme that specifically cleaves single-stranded DNA. Nature 344:467–468
11. Miyake Y, Togashi H, Tashiro M, Yamaguchi H, Oda S, Kudo M, Tanaka Y, Kondo Y, Sawa R, Fujimoto T, Machinami T, Ono A (2006) MercuryII-mediated formation of thymine-HgII-thymine base pairs in DNA duplexes. J Am Chem Soc 128:2172–2173
12. Pelossof G, Tel-Vered R, Liu XQ, Willner I (2011) Amplified surface plasmon resonance based DNA biosensors, aptasensors, and Hg^{2+} sensors using hemin/G-quadruplexes and Au nanoparticles. Chem Eur J 17:8904–8912
13. Li D, Wieckowska A, Willner I (2008) Optical analysis of Hg^{2+} ions by oligonucleotide–gold-nanoparticle hybrids and DNA-based machines. Angew Chem Int Ed 47:3927–3931
14. Kim JS, Quang DT (2007) Calixarene-derived fluorescent probes. Chem Rev 107:3780–3799
15. Zuo X, Song S, Zhang J, Pan D, Wang L, Fan CA (2007) A target-responsive electrochemical aptamer switch (TREAS) for reagentless detection of nanomolar ATP. J Am Chem Soc 129:1042–1043
16. Martinez AW, Phillips ST, Butte MJ, Whitesides GM (2007) Patterned paper as a platform for inexpensive, low-volume, portable bioassays. Angew Chem Int Ed 46:1318–1320
17. Martinez AW, Phillips ST, Carrilho E, Thomas SW III, Sindi H, Whitesides GM (2008) Three-dimensional microfluidic devices fabricated in layered paper and tape. Anal Chem 80:3699–3707
18. Bruzewicz DA, Reches M, Whitesides GM (2008) Low-cost printing of poly (dimethylsiloxane) barriers to define microchannels in paper. Anal Chem 80:3387–3392
19. Carrilho E, Martinez AW, Whitesides GM (2009) Understanding wax printing: a simple micropatterning process for paper-based microfluidics. Anal Chem 81:7091–7095
20. Li X, Tian J, Nguyen T, Shen W (2008) Paper-based microfluidic devices by plasma treatment. Anal Chem 80:9131–9134
21. Chitnis G, Ding Z, Chang CL, Savran CA, Ziaie B (2011) Laser-treated hydrophobic paper: an inexpensive microfluidic platform. Lab Chip 11:1161–1165
22. Wang SM, Ge L, Song XR, Yu JH, Ge SG, Huang JD, Zeng F (2012) Paper-based chemiluminescence ELISA: Lab-on-paper based on chitosan modified paper device and wax-screen-printing. Biosens Bioelectron 31:212–218
23. Xu CX, Li YY, Tian F, Ding Y (2010) Dealloying to nanoporous silver and its implementation as a template material for construction of nanotubular mesoporous bimetallic nanostructures. Chem Phys Chem 11:3320–3328
24. Xu CX, Liu YQ, Su F, Liu AH, Qiu HJ (2011) Nanoporous PtAg and PtCu alloys with hollow ligaments for enhanced electrocatalysis and glucose biosensing. Biosens Bioelectron 27:160–166
25. Yan M, Ge L, Gao WQ, Yu JH, Song XR, Ge SG, Jia ZY, Chu CC (2012) Electrogenerated chemiluminescence from a phenyleneethynylene derivative and its ultrasensitive immunosensing application using a nanotubular mesoporous Pt–Ag alloy for signal amplification. Adv Funct Mater 22:3899–3906
26. Hermanson GT (2008) Bioconjugate techniques, 2nd edn. Elsevier, Rockford
27. Noh HB, Rahman MA, Yang JE, Shim YB (2011) Ag (I)-cysteamine complex based electrochemical stripping immunoassay: ultrasensitive human IgG detection. Biosens Bioelectron 26:4429–4435
28. Wang SM, Ge L, Song XR, Yan M, Ge SG, Yu JH, Zeng F (2012) Simple and covalent fabrication of a paper device and its application in sensitive chemiluminescence immunoassay. Analyst 137:3821–3827
29. Tan YH, Davis JA, Fujikawa K, Ganesh NV, Demchenko AV, Stine KJ (2012) Surface area and pore size characteristics of nanoporous gold subjected to thermal, mechanical, or surface modification studied using gas adsorption isotherms, cyclic voltammetry, thermogravimetric analysis, and scanning electron microscopy. J Mater Chem 22:6733–6745
30. Yuan C, Zhang K, Zhang Z, Wang S (2012) Highly selective and sensitive detection of mercuric ion based on a visual fluorescence method. Anal Chem 84:9792–9801
31. Du J, Liu M, Lou X, Zhao T, Wang Z, Xue Y, Zhao J, Xu Y (2012) Highly sensitive and selective chip-based fluorescent sensor for

mercuric ion: development and comparison of turn-on and turn-off systems. Anal Chem 84:8060–8066
32. Huang D, Niu C, Wang X, Lv X, Zeng G (2013) "Turn-on" fluorescent sensor for Hg^{2+} based on single-stranded DNA functionalized Mn: CdS/ZnS quantum dots and gold nanoparticles by time-gated mode. Anal Chem 85:1164–1170
33. Han D, Kim Y, Oh JW, Kim TH, Mahajan RK, Kim JS, Kim H (2009) A regenerative electrochemical sensor based on oligonucleotide for the selective determination of mercury (II). Analyst 134:1857–1862
34. Aragay G, Pons J, Merkoc A (2011) Enhanced electrochemical detection of heavy metals at heated graphite nanoparticle-based screen-printed electrodes. J Mater Chem 21:4326–4331